Desalination and Water Treatment
www.deswater.com
doi: 10.5004/dwt.2021.27111

223 (2021) 363–379
May

Removal of reactive blue and disperse red dyes from synthetic textile effluent by electrocoagulation process using Al–Al and Fe–Fe electrodes: parametric optimization by response surface methodology

Noufissa Sqalli Houssini*, Abdelhafid Essadki*, Esseddik Elqars

Laboratory of Environment, Process, Energy (LEPE), Hassan II University, Ecole Supérieure de Technologie, BP. 8012 Oasis, Casablanca, Morocco, Tel. +212642496324; email: noufissa.sqalli@gmail.com (N.S. Houssini), Tel. +212619191929; email: essadkiha@gmail.com (A. Essadki), Tel. +212661118266; email: s.elqars@gmail.com (E. Elqars)

Received 14 September 2020; Accepted 4 February 2021

ABSTRACT

This study deals with the treatment of synthetic effluent containing two textile dyes (reactive blue and disperse red 74) by electrocoagulation (EC) using iron electrodes. Then the results are compared with the performance of aluminum electrodes. Response surface methodology using the JMP.11 statistical experimental design was performed to design experiments and to optimize the process. Twenty experiments were conducted to study the effect of four important process parameters: current density (5–25 mA/cm^2), initial pH (4–11), electrolyte concentration (1–5 g/L), and operating time (20–60 min) for the color removal efficiency (CRE) and consumption energy (CE). The parameters for maximum CRE and minimum CE were found with iron electrodes at current density 17.08 mA/cm^2, operating time 20 min, pH 9, and electrolyte concentration 2 g/L, for aluminum at 25 mA/cm^2, pH 4, operating time 60 min, and electrolyte concentration 2.5 g/L. Reactive and disperse dyes treated with iron electrodes shows efficiency in terms of color removal in alkaline solutions, compared with aluminum electrodes, and more efficiency was obtained in acidic solutions. The operating cost was calculated by considering the energy and electrode consumption and evaluated as 83.879 \$/m^3 of treated wastewater for iron electrodes and 126.23 \$/m^3 of treated wastewater for aluminum electrodes. SEM analysis was performed in further study and show the efficiency of the electrocoagulation process in dye removal. The findings of this study show also that chemical analysis and RSM are suitable for investigating the mechanism and optimization of EC as applied to textile effluents.

Keywords: Electrocoagulation process; Iron electrodes; Aluminum electrodes; Removal efficiency; Experimental design

1. Introduction

Textile wastewater is one of the most polluted wastewaters and has been a serious environmental problem [1,2]. It is estimated that for each ton of finished textile product, 1 million tons of dyes are produced per year and approximately 200–350 m^3 of colored wastewater is released to aquatic streams [3]. The textile effluents are highly contaminated and contain different kinds of organic and inorganic pollutants, heavy metals, and colorants [4]. Therefore, such wastewater is characterized by strong color, high amounts of total dissolved solids (TDS), high chemical oxygen demand (COD), highly fluctuating pH (2–12), and low biodegradability, with a 5 d biochemical oxygen demand/COD of less than 0.25 [5,6]. The presence of synthetic dyes leads to the recalcitrance of textile effluents [7]. Table 1 shows the characteristics of the synthetic effluent used in this study.

Heavy metal-containing dyes which are used extensively in the textile industry are toxic, potentially carcinogenic, and have caused serious environmental pollution [8], since

* Corresponding authors.

Table 1
Characteristics of the synthetic effluent used

Character	Value
Turbidity (NTU)	326
Color (reactive and disperse dyes) (mg/L)	40
Conductivity (mS/cm)	2–3
pH	7.3–7.8

the complex aromatic structures of the organic dyes are resistant to light, biological activity, and other degradative environmental conditions [9,10]. They are composed of a group of atoms responsible for their color, which is called the chromophore, as well as an electron-withdrawing or donating substituent that influences the color of the chromophore, called the auxochrome [11]. Dyes are classified based on their chemical structures, physical properties, and applications in various processes. Moreover, the major classification of synthetic dyes normally used includes anthraquinone, indigoide, triphenylmethyl, xanthene, and azo derivatives [12,13]. Among different groups of dyes, azo dyes are the most common synthetic dyes that are widely used in the textile industry. In fact, azo dyes make up 60%–70% of all dyes, azo dyes contain xenobiotic substitutions, including azo, sulfonic acid, nitro, chloro, and bromo functional groups [14,6]. Dyes can also be classified according to their usage, such as reactive, disperse, direct, vat, sulfur, cationic, acid, mordant, ingrain, and solvent dyes that are listed in the color index (C.I.) by the Society of Dyers and Colorists and the American Association of Textile Chemists and Colorists.

Conventionally, textile wastewater is treated by various methods, such as biological methods, adsorption, chemical degradation, advanced oxidation processes, and chemical coagulation [15–17]. Biological methods cannot be applied to most textile wastewaters due to the toxicity of most commercial dyes to the organisms used in the process [18,19]. Adsorption has the associated cost and difficulty of the regeneration process and a high waste disposal cost [20]. Chemical degradation produces some very toxic products such as organochlorine compounds [21]. Advanced oxidation processes such as ozonation, UV, and ozone-UV combined oxidation, photocatalysis, Fenton reactive, and ultrasonic oxidation are not economically feasible [20] and chemical coagulation has been found to be robust, cost-effective, easy to operate, and energy-saving treatment options [22] but it causes extra pollution due to the undesired reactions in treated water and produces large amounts of sludge [9].

Research on wastewater treatment has centered on electrochemical coagulation as it is simple to operate with less amount of sludge [8]. Electrocoagulation process has been used for wastewater treatment for its moderate requirement of chemicals, versatility, safety, selectivity, ease of control, and automation [23]. It is a simple and efficient method where the flocculating agent is generated in situ by electro-oxidation of a sacrificial anode [24]. Electrocoagulation process has been applied to treat textile wastewaters [25–27], dyes [28–30]. The most widely used electrode materials in the electrocoagulation process are aluminum and iron [31–33]. Generally, the aluminum electrode is used in an acidic medium (pH < 6), whereas, a neutral and alkaline medium is more suitable for the iron electrode [34–36].

The EC process can be summarized in three steps [37,38]: (i) comprising of dissolution; electrolytic reactions at electrode surfaces, (ii) coagulation, formation of coagulants in an aqueous phase, (iii) flocculation; adsorption of soluble or colloidal pollutants on coagulants, and removal by sedimentation.

In the EC process, *in-situ* generation of metal hydroxide $Al(OH)_3$ and $Fe(OH)_3$ occurs due to the dissolution of sacrificial aluminum or iron anodes in water which acts as a coagulant and the reduction of water at the cathode via reactions (1)–(4), [39].

Anode reaction:

$$Al \rightarrow Al^{3+}_{(aq)} + 3e^- \quad (1)$$

$$Fe \rightarrow Fe^{2+}_{(aq)} + 2e^- \quad (2)$$

$$Fe^{2+}_{(aq)} \rightarrow Fe^{3+} + e^- \quad (3)$$

Cathode reaction:

$$3H_2O + 3e^- \rightarrow \frac{3}{2}H_2 + 3OH^- \quad (4)$$

Al^{3+}, Fe^{3+}, and OH ions, generated via the electrode reactions mentioned above, will react to form various hydroxides and/or polyhydroxides species in the reaction medium (such as $Al(OH)^{2+}$, $Al(OH)^{+}_2$, $Fe(OH)_2$ hydroxide species; $Al_6(OH)^{3+}_{15}$, $Al_8(OH)^{4+}_{20}$, $Al_{13}(OH)^{5+}_{34}$; $Fe(H_2O)^{2+}_6$, $Fe_2(H_2O)_8(OH)^{4+}_2$… polyhydroxides species) depending on the pH range of the media. At pH 4–9.5, these species are transformed into $Al(OH)_{3(s)}$ and $Fe(OH)_{2(s)}$, respectively, through complex precipitation reactions (5) and (6) [40]:

$$Fe^{3+}_{(aq)} + 3H_2O \rightarrow Fe\left(OH\right)_{3(s)} + 3H^+_{(aq)} \quad (5)$$

$$Al^{3+}_{(aq)} + 3H_2O \rightarrow Al\left(OH\right)_{3(s)} + 3H^+_{(aq)} \quad (6)$$

Freshly formed amorphous $Fe(OH)_{3(s)}$ and $Al(OH)_{3(s)}$ flocks are beneficial for the rapid adsorption of soluble or colloidal organic and inorganic compounds on coagulants and removal by sedimentation or flotation [39].

The recent studies highlight the importance of further investigating the application of EC treatment processes to textile effluents containing different classes of dyes, simultaneously optimizing the operating conditions, through the use of the response surface methodology (RSM), it showed excellent advantages of optimization compared with the traditional method by reducing experimental trials to provide sufficient information for statistically right results and valuation of the proportional significance of parameters and their interactions [41].

The aim of this present work is to identify the optimal operating conditions for the electrocoagulation process such as (current density, pH, electrolyte concentration, and

operating time), then to study the color removal from synthetic effluent of two textile dyes (reactive blue and disperse Red 74) and the consumption energy as system responses, first using iron electrodes then results were compared with aluminum electrodes.

2. Materials and methods

The electrocoagulation set-up is schematically shown in Fig. 1. The electrocoagulation reactor consisted of a double-walled Pyrex batch EC cell with 5 L capacity of synthetic effluent, a propeller stirrer of length (h = 6 cm) was placed in the middle of the compartment at 4 cm from the bottom of the reactor with at constant stirring speed (100 rpm). The temperature of the solution has been monitored to the desired value with a digital thermostat as a thermostatic bath (Ultratemp 2000). Two iron or aluminum plates (pure aluminum and E24 iron) of area 70 cm^2 were used as anode and cathode electrodes at an inter-electrode distance of 1 cm. The aluminum (or iron) electrodes were connected to a power generator (BK precision) to control current density. Working electrode surfaces were abraded through silicon carbide metallurgical paper degreased in acetone and then dried [41].

The pH of the solution was measured by a pH meter Crison Instruments, s.a, Barcelone, Espagne and adjusted by adding diluted NaOH or HCl solutions. The conductivity of the solution was measured by conductivity-meter (CRISON EC-meter BASIC 30+) and wad adjusted by adding Sodium chloride solution.

The color evolution was monitored by absorbance measurement using a UV-visible spectrophotometer (HEλIOS) with two wavelengths of 569 and 600 nm corresponding to the maximum absorbance of respectively disperse and reactive dyes. Samples containing the same concentrations for both types of dyes were prepared. Absorbance for different concentrations was measured for both wavelengths to study the evolution of each type of dye. A linear evolution between concentration and absorbance was obtained.

Reactive blue and disperse Red 74 were obtained from the textile industry based in Casablanca, their chemical structures are illustrated in Figs. 2 and 3. Synthetic effluent was prepared by dissolving dyes (40 mg/L) as per the reported dyes concentration of real textile wastewater in tap water.

Color is expressed as:

$$Y(\mathrm{COL})\% = \frac{A_0 - A}{A_0} \times 100 \tag{7}$$

where A_0 and A are, respectively, the initial absorbance and the absorbance at a certain time.

Sludge samples were analyzed by EDAX coupled with scanning electron microscopy (SEM) using Thermo Fisher Scientific Inc., (Waltham, Massachusetts, U.S.) Quatro S, to quantify the elemental composition.

2.1. Cost analysis

Cost analysis plays an important role in industrial wastewater treatment techniques as the wastewater treatment technique should have cost attractive. In this preliminary economic study, energy consumption (kWh/m^3), electrode material (kg/m^3), and supporting electrolyte concentration (SEC) (kg/m^3) costs are taken into account as major cost items and were calculated for different electrode materials (iron and aluminum). Sludge treatment was not done in this study, just sampling for SEM analysis. Therefore, the cost of sludge disposal will be evaluated in future study. The operating cost of electrocoagulation was calculated by Eq. (8) [42], unit prices, a, b, and c gave for Morocco Market (National Office of Electricity, SONASID):

Fig. 1. Experimental setup of electrocoagulation process.

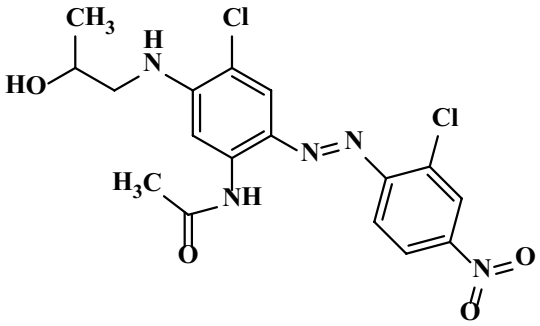

Fig. 2. Molecular structure of disperse Red 74 (569 nm).

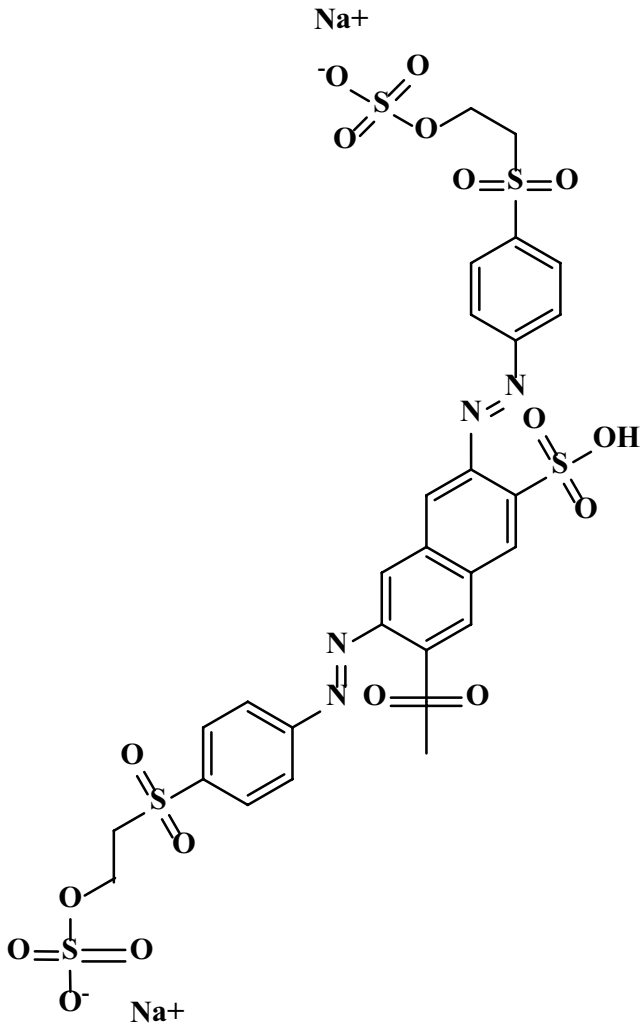

Fig. 3. Molecular structure of reactive Blue (600 nm).

$$\text{Operating cost} = a \times E(\text{kWh/kg}) + b \times \Delta m_{\text{experimental}} + c \times \text{SEC}\left(\text{kg/m}^3\right) \quad (8)$$

The specific electrical energy consumption as kWh/m^3 was calculated as follows [43]:

$$E = \frac{U \times I \times t}{V \times Y\%} \quad (9)$$

where U (V) cell voltage; I (A) current intensity; t (h) electrolysis time; V (L) liquid volume, and Y dye removal efficiency.

The consumption energy as kWh/kg of removed dyes was calculated for optimization using statistical analysis, and as kWh/m^3 of synthetic effluent to evaluate cost analysis.

The mass loss of the sacrificial anodes obtained experimentally was calculated as follows:

$$\Delta m_{\text{experimental}} = m_i - m_f \quad (10)$$

where m_i (g) is the initial mass of the anode before treatment and m_f (g), if the final mass measured after the electrocoagulation process.

Faraday's law (Eq. (11)) predicts the theoretical electrochemical mass losses. Therefore, to evaluate the operating cost, we have used the experimental amount of anodic dissolution.

The quantity of material produced and consumed during an electrochemical reaction is calculated by Faraday's law [10]:

$$\Delta m_{\text{theoritical}} = \frac{I \times t \times M}{n \times F} \quad (11)$$

where I (A) is the current intensity; t (s) is the electrolysis time, M is the molecular weight from Al (26.98g/mol), and Fe (55.84g/mol), n is the number of electrons transferred (Al: n = 3; Fe: n = 3) and F: Faraday constant = 96,485.3 C/mol.

2.2. Experimental design

The experimental runs were designed using John Macintosh Project.11 (JMP.11) software performed for regression and graphical analysis of obtained data. Optimal design and ANOVA analysis under RSM were chosen as a model of optimization. The RSM is the most common technique used in industrial research, particularly in situations where a large number of variables influencing the system features [44]. The validation of the model is considered adequate if the variance due to regression is different from the total variance (ANOVA) [45].

The main operational parameters were current density (5–25 mA/cm^2), initial pH (4–11), electrolyte concentration (1–5 g/L), and operating time (20–60 min). Color removal efficiency (CRE) and consumption energy were considered as responses.

The factors were coded as given by Eq. (12):

$$X_i = \frac{x_i - x_0}{\Delta x} \quad (12)$$

The behavior of the system is explained by the following quadratic equation [46]:

$$y = a_0 + a_1 \times x_1 + \ldots a_n \times x_n + \sum_{i,j=1 i \neq j}^{n} a_{ij} \times x_i \times x_j + \sum_{i,j,k=1 i \neq j \neq k}^{n} a_{ijk} \times x_i \times x_j \times x_k + \ldots \quad (13)$$

where y is the theoretical response function; X_j is the coded variables of the system; a_0, a_{ij}, a_{ijk} is the true model coefficients.

3. Results and discussions

3.1. Statistical analysis using iron electrodes

In the present study, preliminary experiments were conducted to determine the most crucial factors and the effective range of these factors using iron electrodes. Four factors were chosen to evaluate and optimize the electrocoagulation treatment process and to study the effect of variables on removal efficiency and energy consumption. Each parameter has two levels: –1 or +1 indicating respectively minimum and maximum. The corresponding four variable central composite designs (CCD) and their responses realized by experiments are shown in Table 2 using JMP1.11 software.

Figs. 4 and 5 show the estimation for removal efficiency and consumption energy. The most important parameters, which affect the efficiency of electrocoagulation are current density and pH crossed the blue line (Prob. < 0.05). Operating time is significant also, electrolyte concentrations were eliminated from the model. Factors are defined linearly in order to study the combined effect of these factors. A second study was done to display the interactions and second-order between process parameters.

The model was enhanced by fixing electrolyte concentration at 2 g/L correspondings to a conductivity of 2.78 mS/cm. Four experiments were added, a total of 16 experiments were performed including four center points to study the interactions between current density, pH, and operating time (Table 3). The full quadratic model for removal efficiency and consumption energy is given by Eqs. (14) and (15), where X_1, X_2, and X_4 are current density, pH, and operating time, respectively:

$$y_1(CRE\%) = 96.819 + 4.2076X_1 + 2.774X_2 + 2.3178X_4 - 1.37X_1^2 - 0.93X_1X_2 - 1.71X_2^2 - 1.26X_1X_4 - 0.54X_2X_4 - 1.35X_4^2 \quad (14)$$

$$y_2(CE) = 23.94 + 16.665X_1 - 4.75X_2 + 2.174X_4 + 6.034X_1^2 - 3.809X_1X_2 - 1.15X_2^2 - 0.075X_1X_4 + 2.046X_2X_4 - 10.35X_4^2 \quad (15)$$

Tables 4 and 5 show regression variance analysis for the two responses. The Fisher's "*F*" test is used to determine the significance of each interaction among the variables, which in turn may indicate the patterns of the interactions among the variables. The significant value of *F* indicates that the most variation in the response can be explained by the regression equation. In general, the larger is the magnitude of *F*, the smaller is the value of *P*, and the more significant is the corresponding coefficient term. A *P*-value lower than 0.01 indicates that the model is considered to be statistically significant [46]. The second-order polynomial model (Eqs. (5) and (6)) is highly significant and adequate to represent the actual relationship between the responses and variables, with a small *P*-value ($P < 0.001$) and a high value of the coefficient of determination ($R^2 = 0.94$ for removal efficiency and $R^2 = 0.88$ for consumption energy).

The 3D response surface and 2D contour plot are generally the graphical representation of the regression equation. Figs. 6 and 7 show the effect of current density and pH on the removal efficiency and consumption energy at fixed values of operating time (40 min) and electrolyte concentration (2 g/L). In the current density range, 18–20 mA/cm^2 and pH range of 7–9, the maximum values of removal efficiency were obtained (94%) and less than 10 kWh/kg of dyes removed. pH is an important operating factor influencing the performance of the electrocoagulation process. The percentage of color removal was increased with increasing pH up to 9.

The study results agree very well with those presented in the literature [47]. The dominant ferric species in the form of $Fe(OH)_{3(s)}$ acts as a coagulating agent, which increases CRE. pH increases the dissolved iron weight during the electrocoagulation process. This increase is due to the formation of iron hydroxide species which adsorb the dye molecules and cause hydrogen evolution at cathodes (Eq. (16)) [48]:

Table 2
Experimental design matrix using central composite design and responses using iron electrodes

Run	Coded values				Real values				Experiments results	
	X_1	X_2	X_3	X_4	Current density (mA/cm^2)	Initial pH	Electrolyte concentration (g/L)	Operating time (min)	Removal efficiency (%)	Consumption energy (kWh/kg of dye removed)
1	–1	–1	–1	–1	10	4	1	20	79.82	5.4
2	1	–1	–1	1	25	4	1	60	93.68	54.74
3	–1	1	1	–1	10	11	5	20	87.62	3.01
4	1	–1	1	–1	25	4	5	20	92.96	53.23
5	–1	1	1	1	10	11	5	60	94.4	8.01
6	–1	1	–1	–1	10	11	1	20	89.73	5.04
7	–1	1	–1	–1	10	11	1	20	97.4	25.28
8	0	0	0	0	17.5	7.5	3	40	97.6	25.99
9	1	1	–1	1	25	11	1	60	98.91	53.21
10	–1	–1	–1	1	10	4	1	60	85.7	15.02
11	1	1	1	1	25	11	5	60	98.35	24.32
12	–1	–1	1	1	10	4	5	60	90.86	6.98

Factors	Estimate	Standard error	t ratio	Prob. > |t|
Current density(10,25)	3,8248913	0,95356	4,01	0,0051*
pH(4,11)	2,5551087	0,95356	2,68	0,0316*
Operating time(20,60)	1,803442	0,95356	1,89	0,1005
Electrolyte concentration(1,5)	0,9732246	0,95356	1,02	0,3414

Fig. 4. Sorted parameters estimation for removal efficiency using iron electrodes.

Factors	Estimate	Standard error	t ratio	Prob. > |t|
Current density(10,25)	17,581455	3,093108	5,68	0,0007*
pH(4,11)	-5,013121	3,093108	-1,62	0,1491
Electrolysis time(20,60)	2,2203786	3,093108	0,72	0,4961
Electrolysis concentration(1,5	-1,623545	3,093108	-0,52	0,6159

Fig. 5. Sorted parameters estimation for consumption energy using iron electrodes.

Table 3
Data matrix of factors and responses of enhanced experimental design using iron electrodes

Run	Coded Values				Real values				Experiments results	
	X_1	X_2	X_3	X_4	Current density (mA/cm^2)	Initial pH	Electrolyte concentration (g/L)	Operating time (min)	Removal efficiency (%)	Consumption energy (kWh/kg of dye removed)
13	0	0	0	–1	17.5	7.5	3	20	92.98	6.86
14	1	–1	0	1	25	4	3	60	98.61	29.9
15	0	1	0	0	17.5	11	3	40	97.71	13.66
16	–1	0	0	0	10	7.5	3	40	91.07	8.94

Table 4
Regression variance analysis for dyes removal efficiency using iron electrodes

Source	Degree of freedom	Sum of squares	Mean square	*F*-statistics	*P*
Model	4	304.086	76.0215		
Residual	7	66.92282	9.5604	7.9517	<0.0001
Total	11	371.00883			

Table 5
Regression variance analysis for consumption energy using iron electrodes

Source	Degree of freedom	Sum of squares	Mean square	*F*-statistics	*P*
Model	4	3,720.7731	930.193		
Residual	7	704.1543	100.593	9.2471	<0.0001
Total	11	4,424.9275			

$$2H_2O + 3e^- \rightarrow H_{2(g)} + 2OH^-_{(aq)} \quad (16)$$

Regarding Pareto graphs (Figs. 8 and 9), the current density variable was the most important factor for CRE and consumption energy using iron electrodes with a 90% effect. the percentage effects of pH and operating time variables were higher than 50%. It is valuable to notify that the high effect of the current density variable on CRE can be due to the synergistic effect of coagulation and oxidation that is increased through more production of $Fe(OH)_3$, this result was also demonstrated by many authors [49].

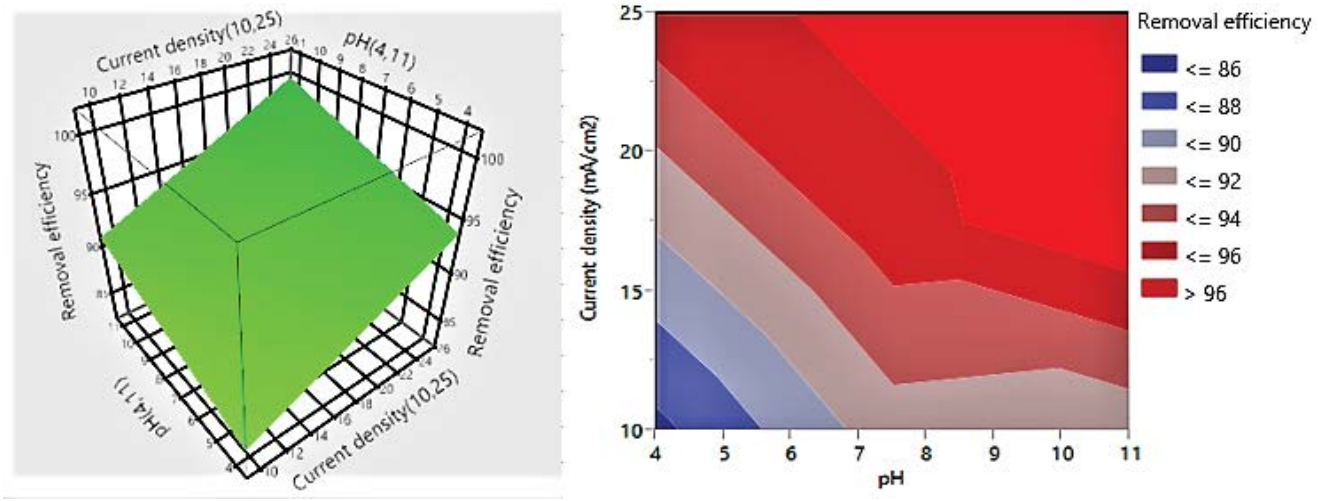

Fig. 6. Response surface plots and 2D contour plots showing the effect of current density and initial pH on removal efficiency at a constant time (40 min) and electrolyte concentration (2 g/L).

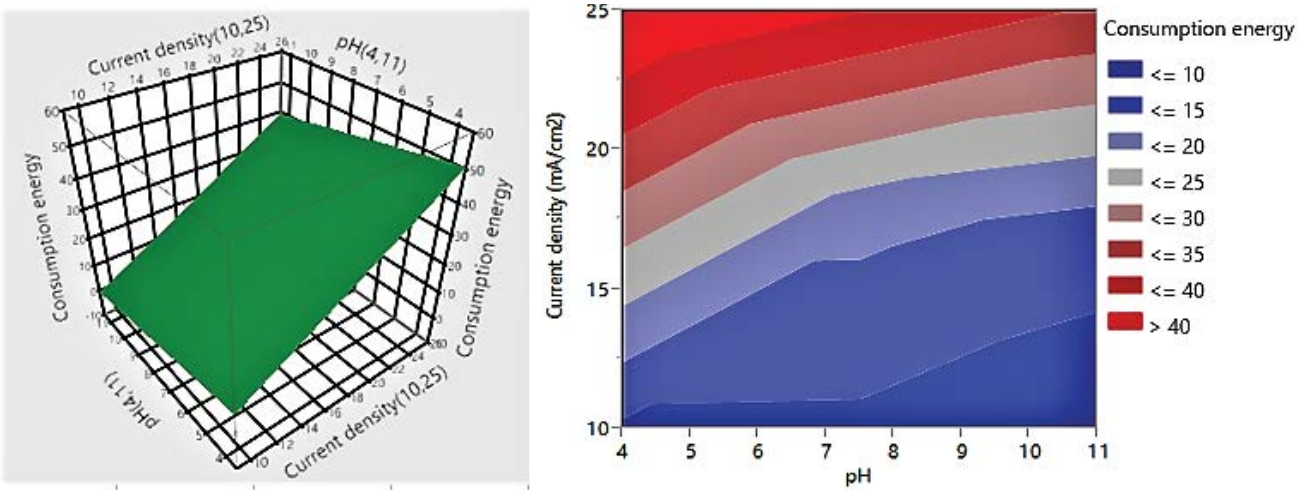

Fig. 7. Response surface plots and 2D contour plots showing the effect of current density and initial pH on consumption energy of dyes at the constant time (40 min) and electrolyte concentration (2 g/L).

3.2. Statistical analysis using aluminum electrodes

The second optimization of the removal of reactive and disperse dyes is achieved using aluminum electrodes as anode and cathode. Twelve experiments are used to estimate the model coefficients. The corresponding four variable CCD are shown in Table 6.

Figs. 10 and 11 show the sorted parameter estimates for removal efficiency and consumption energy. The most important parameters which affect the efficiency of electrocoagulation are pH and current density (values of Prob less than 0.05), operating time affect consumption energy and electrolyte concentration was eliminated from the model. Factors are defined linearly. Furthermore, electrolyte concentration was fixed at 2.5 g/L correspondings to a conductivity equal to 3.32 mS/cm and four experiments were performed to display the interactions and second-order between process parameters (current density, pH, operating time) (Table 7).

The regression model equations (second-order polynomial) relating the three parameters are developed and are given in Eqs. (17) and (18) respectively.

For removal efficiency (%):

$$y_1(CRE\%) = 86.89 + 6.29X_1 - 9.59X_2 + 2.05X_4 + 3.12X_1X_2 - 1.05X_1X_4 + 1.75X_2X_4 - 4.94X_1^2 - 3.01X_2^2 + 3.94X_4^2 \quad (17)$$

For consumption energy (kWh/kg removed dyes):

$$y_2(CE) = 8.43 + 9.32X_1 - 0.95X_2 + 5.27X_4 - 1.13X_1X_2 + 3.6X_1X_4 - 4.24X_2X_4 - 2.53X_1^2 + 4.24X_2^2 + 5.72X_4^2 \quad (18)$$

According to the ANOVA (Tables 8 and 9), the *F*-statistics values for all regression are higher, *p*-values of the model is less than 0.01 indicating that model terms are significant. This means that the terms in the regression equation

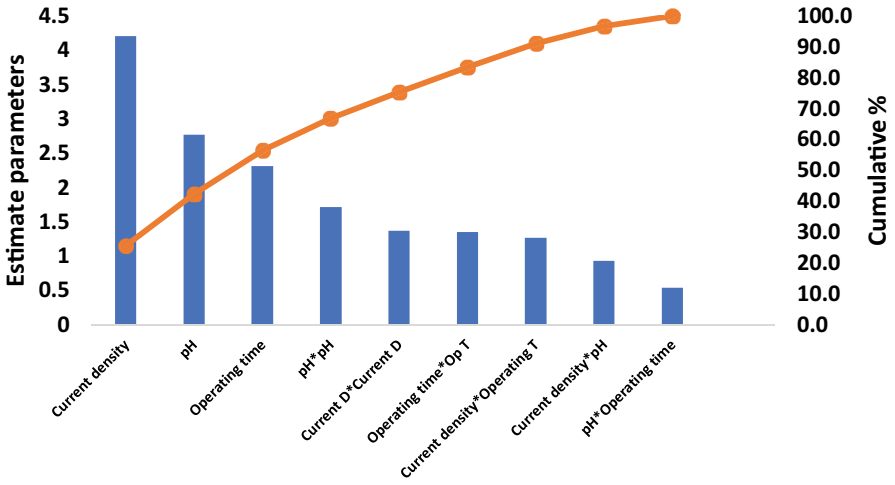

Fig. 8. Pareto graph of the percentage effect of each parameter on the removal efficiency using iron electrodes.

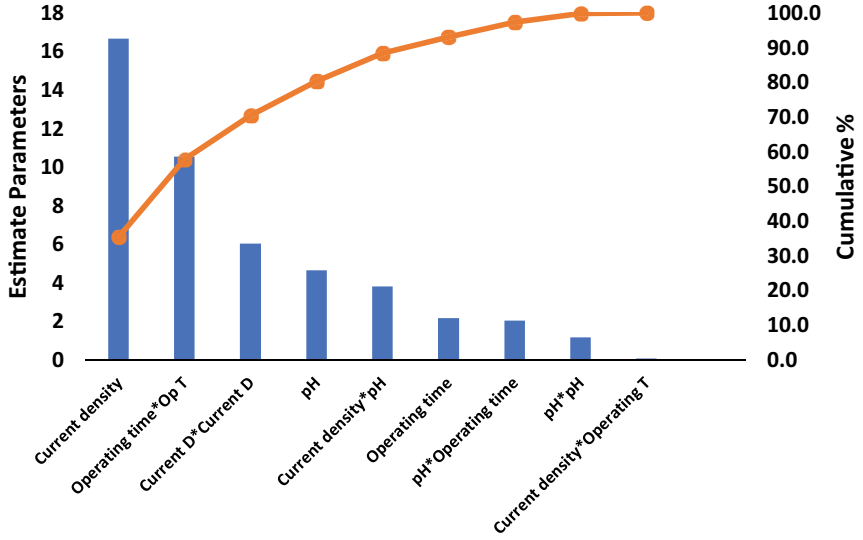

Fig. 9. Pareto graph of the percentage effect of each parameter on the consumption energy using iron electrodes.

have a significant correlation with the response variable. Furthermore, the value of R^2 for CRE is 0.83 and for consumption energy, R^2 = 0.85, the high R^2 value indicates the suitability of the model and the success of the RSM.

Figs. 12 and 13 are surface plots and contour plots show the effect of the studied process parameters on removal efficiency and consumption energy. The pH has an important impact, being in acidic conditions, the removal efficiency increases with decreasing pH and increasing operating time. Moreover, the quantity of dissolved aluminum in solution increases and the electrocoagulation process is more effective [46]. High efficiency was obtained with an initial pH value of 4.5. Furthermore, the superior coagulant is $Al(OH)_3$ in this pH, having a large area to absorb pollutants such as dyes molecules [50]. Thus, maximum decolorization was achieved at 90%.

Fig. 13 shows the interaction effect of current density and operating time at fixed values of the pH (4.5). The consumption energy increased from 15 kWh/kg removed dyes to 30 kWh/kg when increasing operating time and current density from 20 to 60 min and from 15 to 25 mA/cm^2, respectively.

The generation of metallic hydroxides depends on the pH of the aqueous solution and the initial pH of the wastewater affects the performance of electrocoagulation, Paerto graph (Fig. 14) shows the importance of pH for CRE with an 80% effect. Also, Fig. 15 shows that the consumption of energy increases with an increase in the operating time and current density 90% and 60% effect, respectively.

3.3. Optimization and validation of process variables

The goals of the optimization of the EC system were to increase the response of the CRE and minimize the consumption energy for the synthetic effluent studied. To solve this optimization, the "desirability function" was maximized.

Figs. 16 and 17 show that multi-response optimization predicts the following parameters: operating time 20 min,

Table 6
Experimental design matrix using central composite design and responses using aluminum electrodes

Run	Coded values				Real values				Experimental results	
	X_1	X_2	X_3	X_4	Current density (mA/cm²)	Initial pH	Electrolyte concentration (g/L)	Operating time (min)	Removal efficiency (%)	Consumption energy (kWh/kg of dye removed)
1	–1	–1	–1	–1	10	4	1	20	88.4	4.25
2	1	–1	–1	1	25	4	1	60	96.58	47.05
3	–1	1	1	–1	10	11	5	20	45.08	6.01
4	1	–1	1	–1	25	4	5	20	95.21	8.2
5	–1	1	1	1	10	11	5	60	70.1	10.35
6	–1	1	–1	–1	10	11	1	20	71.42	6.18
7	1	1	–1	–1	25	11	1	20	80.4	22.28
8	0	0	0	0	17.5	7.5	3	40	88.14	10.22
9	1	1	–1	1	25	11	1	60	87.43	25.5
10	–1	–1	–1	1	10	4	1	60	95.12	13.52
11	1	1	1	1	25	11	5	60	83.24	26.42
12	–1	–1	1	1	10	4	5	60	85.96	7.45

Factors	Estimate	Standard error	t ratio	Prob. > |t|
pH(4,11)	-9,548243	2,31191	-4,13	0,0044*
Current density(10,25)	6,4799094	2,31191	2,80	0,0264*
Electrolysis concentration(1,5)	-4,065091	2,31191	-1,76	0,1221
Electrolysis time(20,60)	3,9117572	2,31191	1,69	0,1345

Fig. 10. Sorted parameter estimation for removal efficiency using aluminum electrodes.

Factors	Estimate	Standard error	t ratio	Prob. > |t|
Current density(10,25)	7,9227717	2,328407	3,40	0,0114*
Electrolysis time(20,60)	5,8322283	2,328407	2,50	0,0407*
Electrolysis concentration(1,5)	-3,913895	2,328407	-1,68	0,1367
pH(4,11)	0,2405616	2,328407	0,10	0,9206

Fig. 11. Sorted parameter estimation for consumption energy using aluminum electrodes.

Table 7
Data matrix of factors and responses of enhanced experimental design using aluminum electrodes

Run	Coded values				Real values				Experimental results	
	X_1	X_2	X_3	X_4	Current density (mA/cm²)	Initial pH	Electrolyte concentration (g/L)	Operating time (min)	Removal efficiency (%)	Consumption energy (kWh/kg of dye removed)
1	0	0	0	1	17.5	7.5	2.5	60	90.41	13.76
2	0	–1	0	0	17.5	4	2.5	40	92.86	12.75
3	1	0	0	0	25	7.5	2.5	40	87.64	17.34
4	0	0	0	–1	17.5	7.5	2.5	20	90.65	13.68

current density 17.082 mA/cm², and pH 9. The predicted removal efficiency was 93.99% and consumption energy was 6.88 kWh/kg of removed dyes at composite desirability of 0.76, using iron electrodes. For aluminum eletrodes: operating time: 20min, current density: 12.96 mA/cm², and pH 4. The predicted removal efficiency was 92.76% and consumption energy was 4.76 kWh/kg removed dyes at composite desirability of 0.92.

Table 8
Regression variance analysis for dyes removal efficiency using aluminum electrodes

Source	Degree of freedom	Sum of squares	Mean square	*F*-statistics	*P*
Model	4	1,909.5942	477.399		
Residual	7	393.3867	56.198	8.4949	<0.001
Total	11	2,302.9809			

Table 9
Regression variance analysis for consumption energy using aluminum electrodes

Source	Degree of freedom	Sum of squares	Mean square	*F*-statistics	*P*
Model	4	1,341.325	335.331		
Residual	7	399.0207	57.003	5.8827	<0.01
Total	11	1,740.3457			

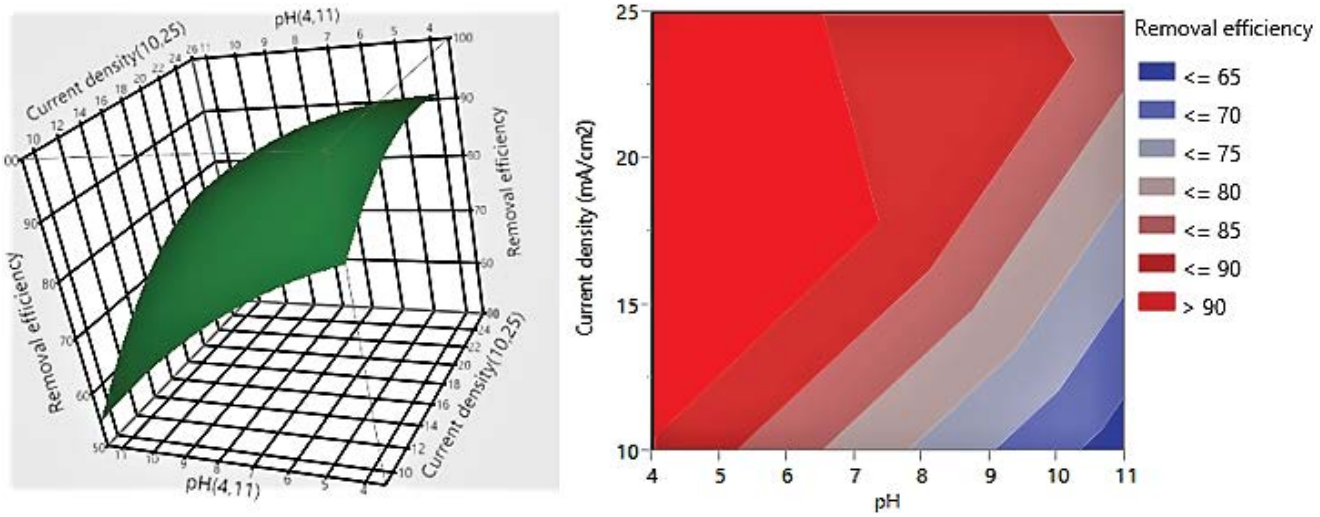

Fig. 12. Response surface plots and 2D contour plots showing the effect of current density and initial pH on removal efficiency at the constant time (40 min) and electrolyte concentration (2.5 g/L).

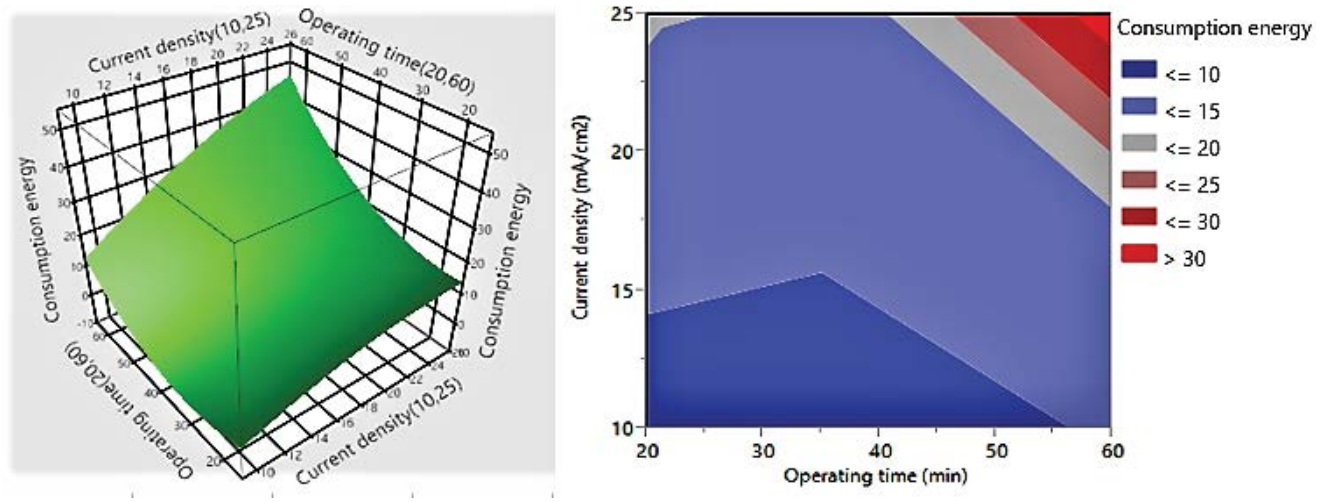

Fig. 13. Response surface plots and 2D contour plots showing the effect of current density and initial pH on removal efficiency of dyes at constant pH 4.5 and electrolyte concentration (2.5 g/L).

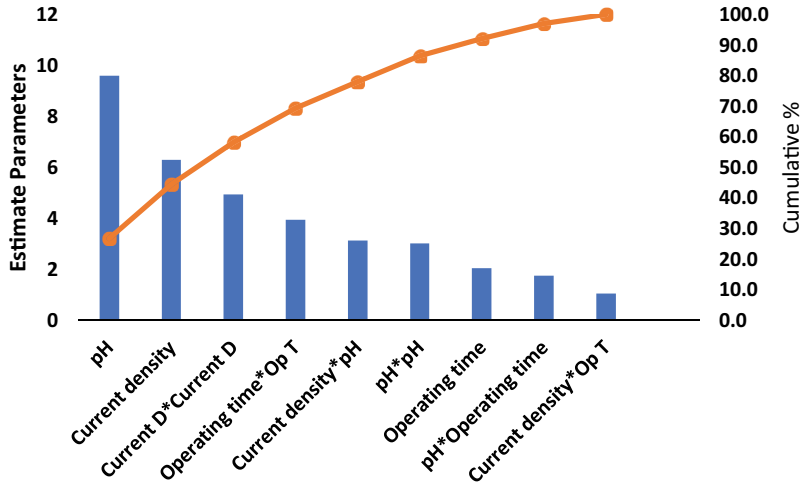

Fig. 14. Pareto graph of the percentage effect of each parameter on the removal efficiency using aluminum electrodes.

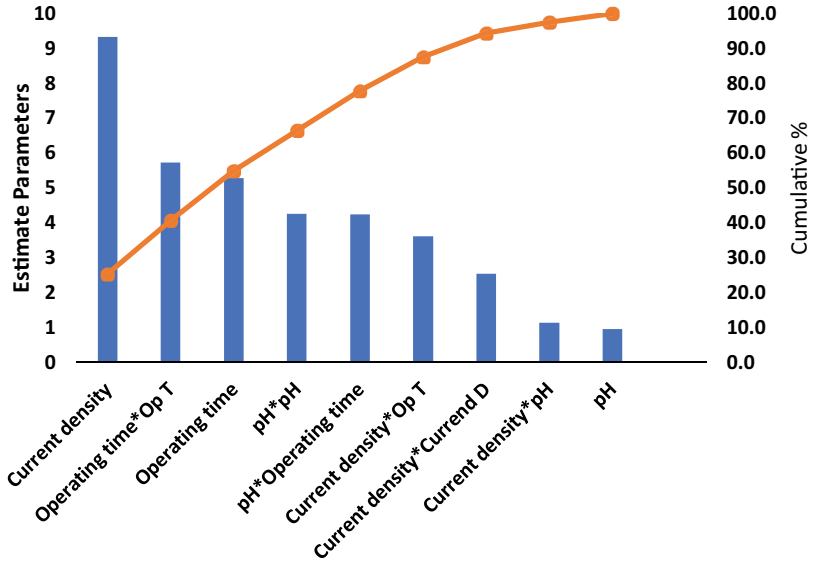

Fig. 15. Pareto graph of the percentage effect of each parameter on the consumption energy using aluminum electrodes.

Thus, the EC process is highly dependent on the initial pH of the wastewater. The generation of metallic hydroxides depends on the pH of the aqueous solution and the initial pH of the wastewater affects the performance of electrocoagulation, Tables 10 and 11 indicate the pH changes during the EC process using iron and aluminum electrodes, respectively.

As in the literature, although the initial pH value was set to 4. for aluminum and 8.9 for iron electrodes, the final pH increased to 6 and to 9.23 at the end of the experiment for aluminum and iron, respectively. The reason for this increase can be explained by the formation of hydrogen gas and the accumulation of hydroxide after the reduction of water in the cathode, confirmed also by many authors [51,52].

This result was experimentally confirmed, we have obtained a removal efficiency of 95% using iron electrodes in alkaline medium and 93% using aluminum electrodes in acid medium with consumption energy of 5.45 kWh/kg of removed dyes and 5 kWh/kg using iron and aluminum respectively. These results are also in agreement with those presented by many researchers, they found that the aluminum electrode is suitable in an acidic medium (pH < 6), whereas, a neutral and alkaline medium is more suitable for the iron electrode [34–36], Bella et al. [53] have proved also that iron anodes were more adequate for reactive and mixture dyes. Chen [35] was confirmed also that iron electrodes allow higher removal efficiency in alkaline medium.

3.4. Sludge analysis

Following the optimization experiments, the sludge was collected, dried in a vacuum oven (T = 120°C), and analyzed by EDAX coupled with SEM using "Thermo scientific Quatro S" for total iron and aluminum content and to further study the interactions of electrocoagulation process.

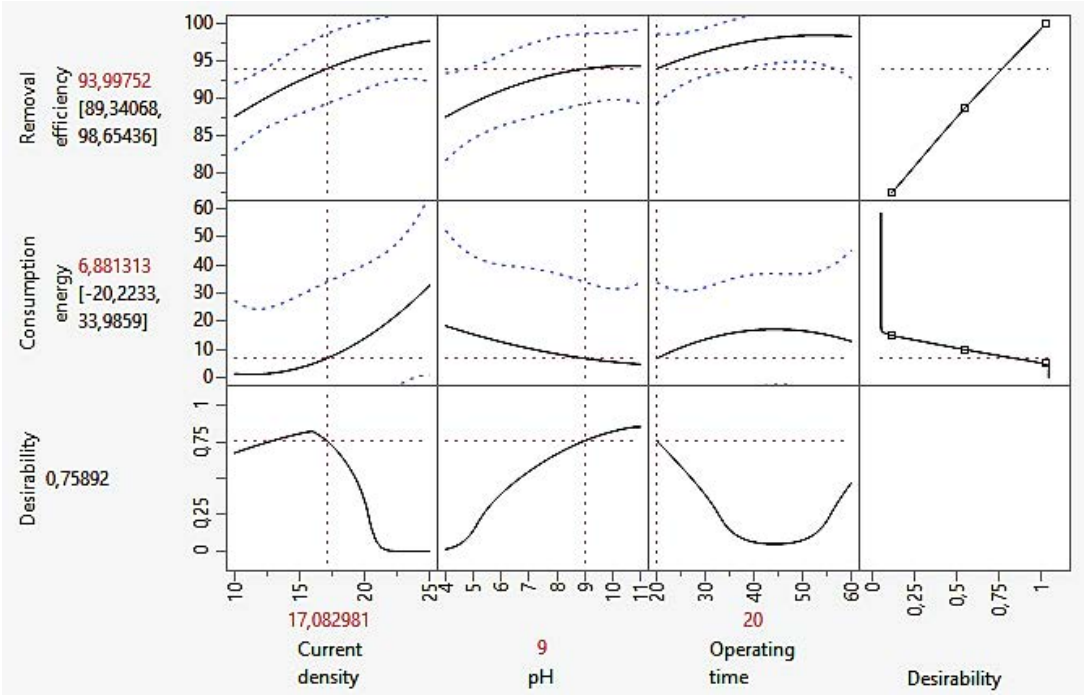

Fig. 16. Multi-response optimization plot for maximizing percentage removal efficiency, and minimizing CE using iron electrodes.

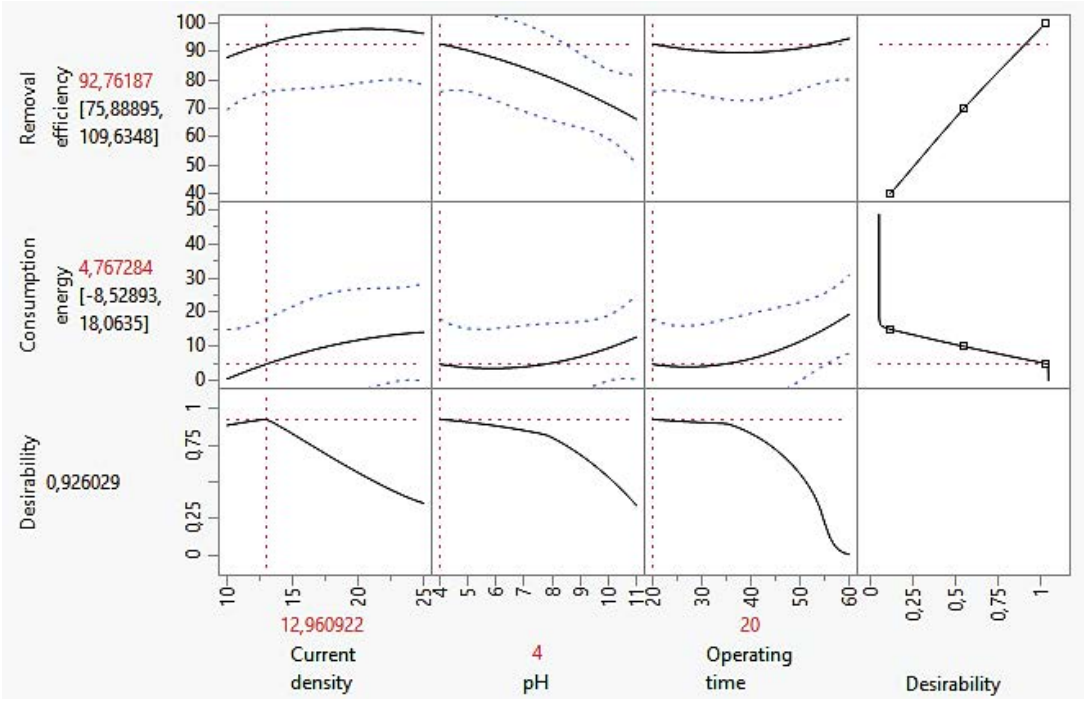

Fig. 17. Multi-response optimization plot for maximizing percentage removal efficiency, and minimizing CE using aluminum electrodes.

EDAX analysis of dried sludge using iron and aluminum electrodes are provided in Figs. 18 and 19, respectively. The EDAX analysis of the sludge indicates the presence of coagulant species such as: sulfur (S); carbon, (C); sodium (Na); oxygen (O); chlorine (Cl), and present in the molecular structure of the dyes. Peaks observed within band range of 900–1,000 cm^{-1} may indicate the presence of S=O group, the group of peaks situated in the range 400–800 cm^{-1} is attributed to the aromaticity or benzene rings [54,55], iron and aluminum are present in the flocs analysis due to the

Table 10
pH evolution during EC process using iron electrodes

Time (min)	pH
0	8.9 (initial pH)
5	9.01
10	9.04
15	9.22
20	9.25

Table 11
pH evolution during EC process using aluminum electrodes

Time (min)	pH
0	4.32 (initial pH)
5	4.66
10	5.18
15	5.89
20	6.24

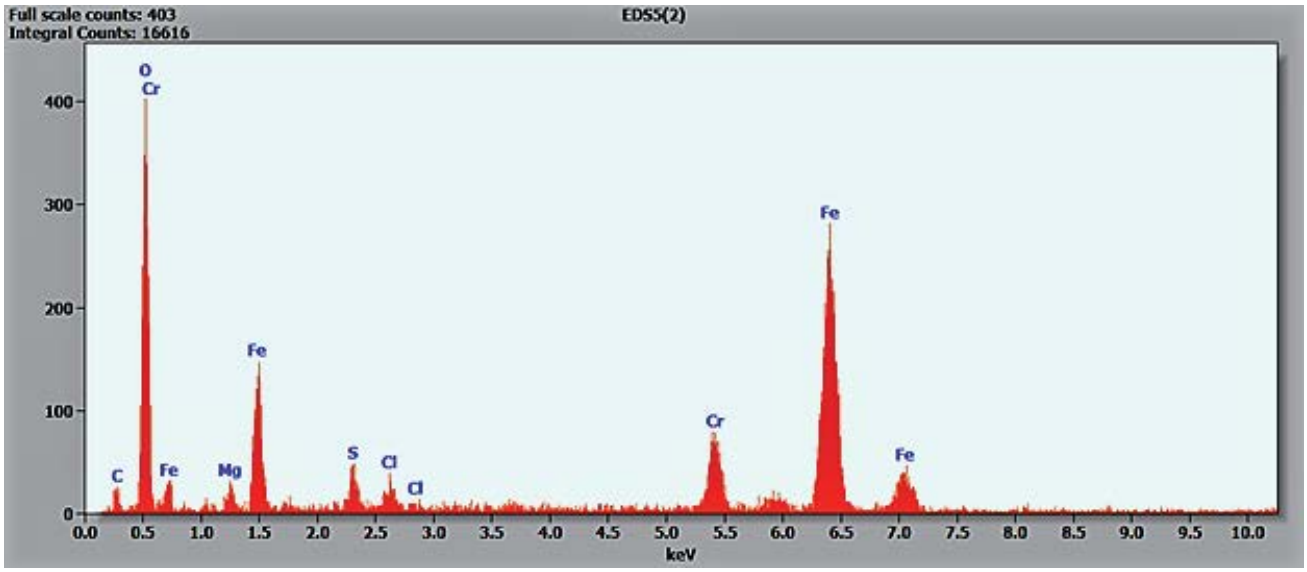

Fig. 18. EDAX spectrum of mixed dyes obtained after electrocoagulation process using iron electrodes (pH = 9; D = 17.08 mA/cm^2; C_{NaCl} = 2 g/L; operating time = 20 min).

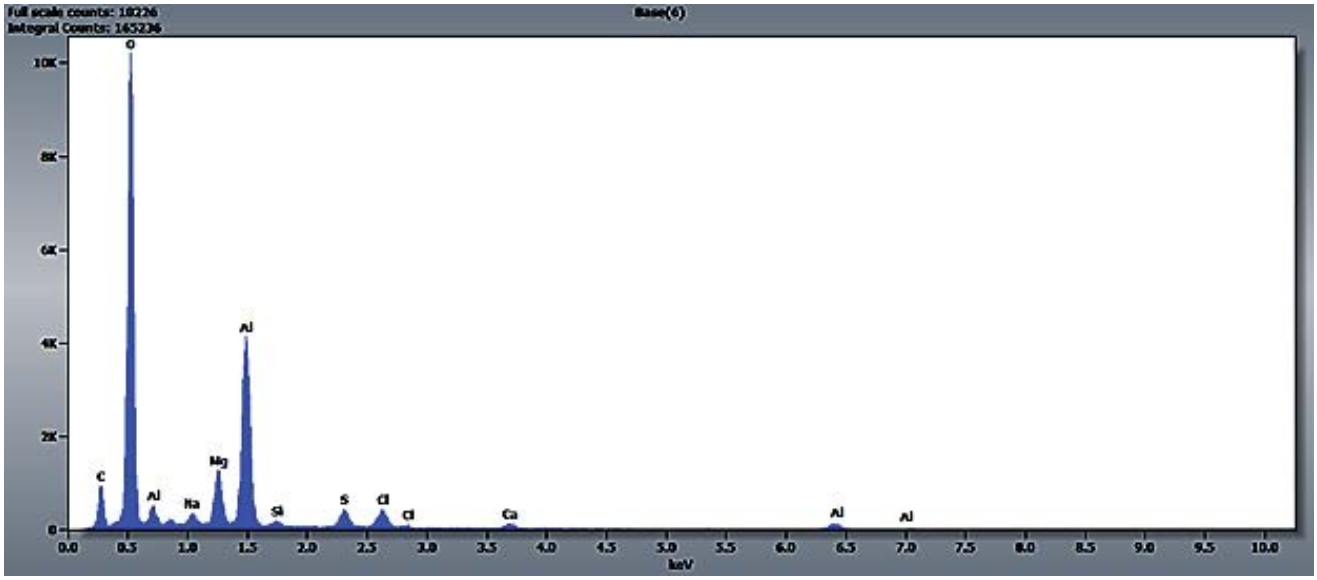

Fig. 19. EDAX spectrum of mixed dyes obtained after electrocoagulation process using aluminum electrodes (pH = 4, D = 12.96 mA/cm^2; C_{NaCl} = 2.5 g/L; operating time = 20 min).

sacrificial anodes. These findings reflect the power of electrocoagulation process to transfer the pollution from water to the formed sludge, as reported by many authors [56].

Weight percentage of iron found by SEM is 48.77%, and aluminum is about 14.48%, which means that the consumption of aluminum sacrificial anode is lower than the iron anode. Furthermore, iron rust faster in salty water, aluminum does not corrode easily, because its surface is protected by a layer of aluminum oxide.

Figs. 20 and 21 show the SEM images of the flocs using iron and aluminum electrodes respectively, it can be observed that flocs are porous and uniform in structure, they are seen as lumpy particles. Uniformity of flocs sizes infers that, produced $Al(OH)_3$ and $Fe(OH)_3$ flocs are coagulated efficiently during the EC process by adequate mixing in the solution. These results are also in agreement with those presented by Das and Kumar Nandi [57].

3.5. Cost analysis of EC process

The treatment of the synthetic effluent using iron and aluminum electrodes was done in the optimal conditions found by the experimental design, Tables 12 and 13 indicate the cost of consumption energy as kWh/m^3 of removed dyes, cost of electrodes consumption using iron and aluminum electrodes respectively and supporting electrolyte cost. It should be noted that all of the economic calculations were based on actual measured metal dissolution values.

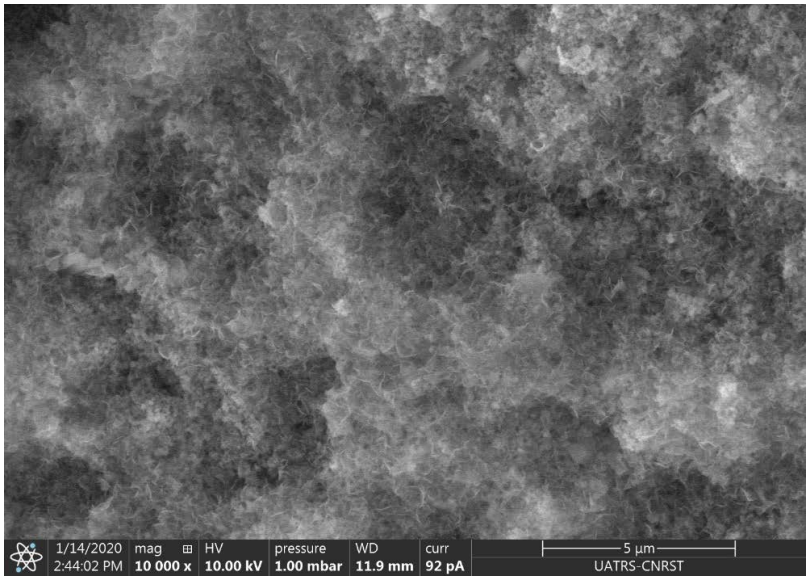

Fig. 20. SEM image of EC produces sludge using iron electrodes in the optimal conditions.

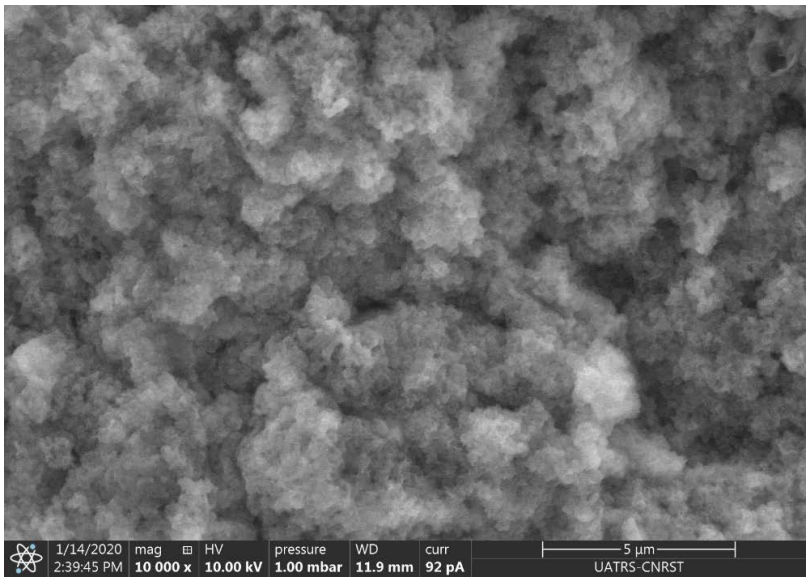

Fig. 21. SEM image of EC produces sludge using aluminum electrodes in optimal conditions.

Table 12
Cost of specific electrical energy and electrodes consumption using iron electrodes

Current density (mA/cm^2)	17.082
Operating time (min)	20
Supporting electrolyte concentration (kg/m^3)	2
E (kWh/m^3)	0.040
Electrical energy price ($/kWh)	0.10
Δm experimental (kg/m^3)	0.176
Δm Faraday (kg/m^3)	0.0328
Electrode material price ($/kg)	1.34
Supporting electrolyte price ($/kg)	41.82

Table 13
Cost of specific electrical energy and electrodes consumption using aluminum electrodes

Current density (mA/cm^2)	12.96
Operating time (min)	20
Supporting electrolyte concentration (kg/m^3)	2.5
E (kWh/m^3)	0.0347
Electrical energy price ($/kWh)	0.10
Δm experimental (kg/m^3)	0.147
Δm Faraday (kg/m^3)	0.012
Electrode material price ($/kg)	147.47
Supporting electrolyte price ($/kg)	41.82

The experimental amount of anodic dissolution is higher than the theoretical amount calculated by Faraday law, this overconsumption of iron and aluminum electrodes is due to the chemical hydrolysis of the cathode, confirmed also by several authors [29,34]. Moreover, this phenomenon is attributed to pitting corrosion especially in the presence of chlorine ions [44] and oxidation of the electrode surface as demonstrated by severals authors, Mameri et al. [58] and Picard et al. [59].

The operating cost of electrocoagulation using iron electrodes was found equal to 83.879 $/m^3 and the operating cost using aluminum electrodes was found equal to 126.23 $/m^3. The operating cost of EC using aluminum electrodes is higher than that using iron electrodes and this is due to their respective prices of each metal (about 1.34 $/kg for iron and 147 $/kg for aluminum. These results are also in agreement with those presented for Al-Fe/EC by many authors [9,60].

Aluminum and iron are the most widely used electrode materials in the electrocoagulation process [32,61] both of them present many advantages and inconvenients: The chemical reaction between Cl− adsorbed on the aluminum oxide film with Al^{3+} species in the oxide lattice promote pitting corrosion that affects the overall dissolution of sacrificial aluminum anode [60], the buffer effect reported for Fe is weaker than for Al. The final pH usually achieved is 9 or 10 with Fe electrodes even when the initial pH is acidic [62,63]. A drawback of iron electrodes (Fe^{2+}) is highly soluble and therefore, not capable of an efficient colloid destabilization by $Fe(OH)_3$, hereby causing poor EC performance.

The aluminum is dissolved in the solution, releasing a transparent color, while the iron emits an ochre to a rust color in powder form, it presents also two additional advantages over aluminum: iron is nontoxic thus it can be used for potable water, even though Moroccan guideline is 200 ppb for aesthetic and organoleptic reasons, which is exactly the same value as for aluminum. The second one is the lower price of iron, about 1.34 $/kg, while aluminum cost lies between 147.47 $/kg.

4. Conclusion

The performance of the electrocoagulation process for the treatment of mixed dyes (reactive blue and disperse red) from the textile industry using iron and aluminum electrodes was investigated. This study has clearly demonstrated that RSM is one of the most common methods to optimize the best-operating conditions to maximize the CRE and to minimize the consumption of energy. The electrocoagulation process was efficient using iron electrodes in basic solutions and using aluminum electrodes in acidic solutions. Furthermore, the optimum value of parameters for high removal efficiency and low consumption energy of removed dyes with Fe–Fe electrodes at pH 9 occurred at current density 17.08 mA/cm^2, operating time 20 min and electrolyte concentration 2 g/L, and with Al–Al electrodes at pH 4, current density 12.96 mA/cm^2, 20 min and electrolyte concentration 2.5 g/L. The total cost at the optimum conditions was calculated as 83.879 $/m^3 for iron electrodes and 126.23 $/m^3 for aluminum electrodes. The SEM analysis of flocs showed that the consumption of aluminum sacrificial anode is lower than the iron anode and reflects the power of the electrocoagulation process to transfer the pollution from water to the formed sludge.

Acknowledgments

This work was supported by Hassan II University of Casablanca for financial help and the National Center for Scientific and Technical Research of Rabat (CNRST) for the technical help.

References

[1] N.M. Mahmoodi, Photocatalytic ozonation of dyes using copper ferrite nano-particle prepared by co-precipitation method, Desalination, 279 (2011) 332–337.
[2] T.H. Kim, C. Park, E.B. Shin, S. Kim, Decolorization of disperse and reactive dyes by continuous electrocoagulation process, Desalination, 150 (2002) 165–175.
[3] S. Arora, Textile dyes: it's impact on environment and its treatment, J. Biorem. Biodegrad., 5 (2014) 484–494.
[4] T.A. Kurniawan, G.Y. Chan, W.-H. Lo, S. Babel, Physico chemical treatment techniques for wastewater laden with heavy metals, Chem. Eng. J., 118 (2006) 83–98.
[5] C. Ramirez, A. Saldana, B. Hernandez, R. Acero, R. Guerraa, S. Garcia-Segura, E. Brillas, J.M. Peralta-Hernández, Electrochemical oxidation of methyl orange azo dye at pilot flow plant using BDD technology, Ind. Eng. Chem. Res., 19 (2013) 571–579.

[6] A. Eslami, M. Moradi, F. Ghanbari, F. Mehdipour, Decolorization and COD removal from real textile wastewater by chemical and electrochemical Fenton processes: a comparative study, J. Environ. Health Sci. Eng., 11 (2013) 1–8.
[7] J.M. Aquino, R.C. Rocha-Filho, L.A.M. Ruotolo, N. Bocchi, Electrochemical degradation of a real textile wastewater using beta-PbO_2 and DSA (R) anodes, Chem. Eng. J., 251 (2014) 138–145.
[8] P. Kalivel, R. Pluto Singh, S. Kavitha, D. Padmanabhan, S. Kumar Krishnan, J. Palanichamy, Elucidation of electrocoagulation mechanism in the removal of Blue SI dye from aqueous solution using Al-Al, Cu-Cu electrodes - A comparative study, Ecotoxicol. Environ. Saf., 201 (2020)813–819.
[9] M. Kobya, M. Bayramoglu, M. Eyvaz, Techno-economical evaluation of electrocoagulation for the textile wastewater using different electrode connections, J. Hazard. Mater., 148 (2007) 311–318.
[10] M. Bayramoglu, M. Kobya, O.T. Can, M. Sozbir, Operating cost analysis of electrocoagulation of textile dye wastewater, Sep. Purif. Technol., 37 (2004) 117–125.
[11] A.B. Dox Santos, F.J. Cervantes, J.B. Van Lier, Review paper on current technologies for decolourisation of textile wastewaters: perspectives for anaerobic biotechnology, Bioresour. Technol., 98 (2007) 2369–2385.
[12] T. Panakoulis, P. Klatzis, D. Kalderis, A. Katsaounis, Electrochemical degradation of Reactive Red 120 using DSA and BDD anodes, J. Appl. Electrochem., 40 (2010) 1759–1765.
[13] Y. Yavuz, R. Shahbazi, Anodic oxidation of Reactive Black 5 dye using boron doped diamond anodes in a bipolar trickle tower reactor, Sep. Purif. Technol., 85 (2012) 130–136.
[14] E. Petrucci, L. Di Palma, R. Lavecchia, A. Zuorro, Treatment of diazo dye Reactive Green 19 by anodic oxidation on a boron-doped diamond electrode, J. Ind. Eng. Chem., 26 (2015) 116–121.
[15] D.T. Sponza, M. Isik, Reactor performance and fate of aromatic amines through decolourization of direct black 38 dye under anaerobic/aerobic sequentials, Process Biochem., 40 (2005) 35–44.
[16] M. Riera-Torres, C. Gutiérrez-Bouzán, M. Crespi, Combination of coagulation–flocculation and nanofiltration techniques for dye removal and water reuse in textile effluents, Desalination, 252 (2010) 53–59.
[17] O.J. Hao, H. Kim, P.C. Chiang, Decolorization of wastewater, Crit. Rev. Environ. Sci. Technol., 30 (2010) 449–505.
[18] N. Mohan, N. Balasubramanian, C.A. Basha, Electrochemical oxidation of textile wastewater and its reuse, J. Hazard. Mater., 147 (2007) 644–651.
[19] Z. Zaroual, M. Azzi, N. Saib, E. Chainet, Contribution to the study of electrocoagulation mechanism in basic textile effluent, J. Hazard. Mater., 131 (2006) 73–78.
[20] O.T. Can, M. Kobya, E. Demirbas, M. Bayramoglu, Treatment of the textile wastewater by combined electrocoagulation, Chemosphere, 62 (2006) 181–187.
[21] N. Daneshvar, A. Oladegaragoze, N. Djafarzadeh, Decolorization of basic dye solutions by electrocoagulation: an investigation of the effect of operational parameters, J. Hazard. Mater., 129 (2006) 116–122.
[22] A.K. Verma, P. Bhunia, R.R. Dash, Supremacy of magnesium chloride for decolourisation of textile wastewater: a comparative study on the use of different coagulants, Int. J. Environ. Sci. Dev., 3 (2012) 119–123.
[23] C. Thakur, V.C. Srivastava, I.D. Mall, Electrochemical treatment of a distillery wastewater: parametric and residue disposal study, Chem. Eng. J., 148 (2009) 496–505.
[24] M. Zaied, N. Bellakhal, Electrocoagulation treatment of black liquor from paper industry, J. Hazard. Mater., 163 (2009) 995–1000.
[25] A. Rauf Shah, H. Tahier, H.M. Kifayatullah, Central composite design based electrocoagulation process for the treatment of textile effluent of S.I.T.E, industrial zone of Karachi City, Desal. Water Treat., 94 (2017) 72–88.
[26] E. Yuksel, M. Eyvaz, E. Gurbulak, Electrochemical treatment of colour index Reactive Orange 84 and textile wastewater by using stainless steel and iron electrodes, Environ. Prog. Sustainable Energy, 32 (2013) 60–68.
[27] U.B. Ogutveren, N. Gonen, S. Koparal, Removal of dye stuffs from wastewater: electrocoagulation of Acilan Blau using soluble anode, J. Environ. Sci. Health., Part A, 27 (1992) 1237–1247.
[28] R. Khosravia, S. Hazratib, M. Fazlzadehb, Decolorization of AR18 dye solution by electrocoagulation: sludge production and electrode loss in different current densities, Desal. Water Treat., 57 (2016) 14656–14664.
[29] A. Maljaei, M. Arami, N.M. Mahmoodi, Decolorization and aromatic ring degradation of colored textile wastewater using indirect electrochemical oxidation method, Desalination, 249 (2009), 1074–7078.
[30] J. Núñeza, M. Yeberb, N. Cisternasc, R. Thibautd, P. Medinab, C. Carrascoa, Application of electrocoagulation for the efficient pollutants removal to reuse the treated wastewater in the dyeing process of the textile industry, J. Hazard. Mater., 371 (2019) 705–711.
[31] T.M. Massara, A.E. Yilmaz, I. Cengiz, S. Malamis, The effect of initial pH and retention time on boron removal by continuous electrocoagulation process, Desal. Water Treat., 112 (2018) 99–105.
[32] X. Zhang, H. Lin, B. Hu, Phosphorus removal and recovery from dairy manure by electrocoagulation, RSC Adv., 6 (2016) 57960–57968.
[33] U. Tezcan, E. Oduncu, Electrocoagulation of landfill leachate with monopolar aluminum electrodes, J. Clean Energy Technol., 2 (2014)15–17.
[34] S. Zodi, O. Potier, F. Lapicque, J.P. Leclerc, Treatment of the textile wastewaters by electrocoagulation: effect of operating parameters on the sludge settling characteristics, Sep. Purif. Technol., 69 (2009) 29–36.
[35] G. Chen, Electrochemical technologies in wastewater treatment, Sep. Purif. Technol., 38 (2004) 11–41.
[36] M. Kobya, T.O. Can, M. Bayramoglu, Treatment of textile wastewaters by electrocoagulation using iron and aluminum electrodes, J. Hazard. Mater., 100 (2003) 163–178.
[37] M.Y.A. Mollah, R. Shennach, J.R. Parga, D.L. Cocke, Electrocoagulation(EC)—science and applications, J. Hazard. Mater., 84 (2001) 29–41.
[38] F. Ozyonar, B. Karagozoglu, Systematic assessment of electrocoagulation for the treatment of marble processing wastewater, Int. J. Environ. Sci. Technol., 9 (2004) 637–646.
[39] F. Ozyonar, O. Gokkus, M. Sabuni, Removal of disperse and reactive dyes from aqueous solutions using ultrasound-assisted electrocoagulation, Chemosphere, 258 (2020) 127325, doi: 10.1016/j.chemosphere.2020.127325.
[40] P. Omwene, M. Kobya, Treatment of domestic wastewater phosphate by electrocoagulation using Fe and Al electrodes: a comparative study, Process Saf. Environ. Prot., 116 (2018) 34–51.
[41] G.E.P. Box, N.R. Draper, Wiley Series in Probability and Mathematical Statistics: Empirical Model-building and Response Surfaces, John Wiley & Sons, Oxford, England, 1987.
[42] D. Ghosh, C.R. Medhi, M.K. Purkait, Techno-economic analysis for the electrocoagulation of fluoride-contaminated drinking water, Toxicol. Environ. Chem., 93 (2011) 424–437.
[43] L. Hongwei, G. Tingyue, L. Yalin, M. Asif, F. Xiong, G. Zhang, Corrosion inhibition and anti-bacterial efficacy of benzalkonium chloride in artificial CO_2-saturated oilfield produced water, Corros. Sci., 117 (2017) 24–34.
[44] K. Atousa Ghaffarian, F. Narges, Treatment of textile dyeing factory wastewater by electrocoagulation with low sludge settling time: optimization of operating parameters by RSM, J. Environ. Chem., 6 (2018) 635–642.
[45] N. Sqalli Houssini, A. Essadki, E. ElQars, The simultaneous removal of reactive and disperse dyes by electrocoagulation process with a bipolar connection of combined iron and aluminum electrodes: experimental design and kinetic studies, Med. J. Chem., 10 (2020) 171–184.
[46] Z. Zaroual, H. Chaair, A.H. Essadki, K. El Ass, M. Azzi, Optimizing the removal of trivalent chromium by

electrocoagulation using experimental design, Chem. Eng. J., 148 (2009) 488–495.
[47] S.H. Ammar, N.N. Ismail, A.D. Ali, W.M. Abbas, Electrocoagulation technique for refinery wastewater treatment in an internal loop split-plate airlift reactor, J. Environ. Chem., 7 (2019) 103489, doi: 10.1016/j.jece.2019.103489.
[48] G.K. Mariah, K.S. Pak, Removal of brilliant green dye from aqueous solution by electrocoagulation using response surface methodology, Mater Today: Proc., 9 (2019) 847, doi: 10.1016/j.matpr.2019.09.175.
[49] M. Ahmadia, F. Ghanbarid, S. Madihi-Bidgoli, Photoperoxi-coagulation using activated carbon fiber cathode as an efficient method for benzotriazole removal from aqueous solutions: modeling, optimization and mechanism, J. Photochem. Photobiol., A, 322 (2016) 85–94.
[50] J.R. Dominguez, T. González, H.M. García, F. Sánchez-Lavado, J.B. de Heredia, Aluminium sulfate as coagulant for highly polluted cork processing wastewaters: removal of organic matter, J. Hazard. Mater., 148 (2007)15–21.
[51] O.T. Can, M. Bayramoglu, M. Kobya, Decolorization of reactive dye solutions by electrocoagulation using aluminum electrodes, Ind. Eng. Chem. Res., 42 (2003) 3391–3396.
[52] O.P. Sahu, V. Gupta, P.K. Chaudhari, V.C. Srivastava, Electrochemical treatment of actual sugar industry wastewater using aluminum electrode, Int. J. Environ. Sci. Technol., 12 (2015) 3519–3530.
[53] W. Balla, A.H. Essadki, B. Gourich, A. Dassaa, H. Chenik, M. Azzi, Electrocoagulation/electroflotation of reactive, disperse and mixture dyes in an external-loop airlift reactor, J. Hazard. Mater., 184 (2010) 710–716.
[54] S. Aoudj, A. Khelifa, N. Drouiche, M. Hecini, H. Hamitouche, Electrocoagulation process applied to wastewater containing dyes from textile industry, Chem. Eng. Process.: Process Intensif., 49 (2010) 1176–1182.
[55] S.-H. Kim, P.-P. Choi, Enhanced Congo red dye removal from aqueous solutions using iron nanoparticles: adsorption, kinetics, and equilibrium studies, Dalton Trans., 46 (2017) 15470–15479.
[56] F.E. Titchou, H. Alfanga, H. Zazou, R.A. Akbour, M. Hamdani, Batch elimination of cationic dye from aqueous solution by electrocoagulation process, Med. J. Chem., 10 (2020) 1–12.
[57] D. Das, B. Kumar Nandi, Removal of Fe(II) ions from drinking water using electrocoagulation (EC) process: parametric optimization and kinetic study, J. Environ. Chem. Eng., 7 (2019), doi: 10.1016/j.jece.2019.103116.
[58] N. Mameri, A.R. Yeddou, H. Lounici, D. Belhocine, H. Grib, B. Bariou, Defluoridation of septentrional Sahara water of North Africa by electrocoagulation process using bipolar aluminium electrodes, Water Res, 32 (1998) 1604–1612.
[59] T. Picard, G. Cathalifaud-Feuillade, M. Mazet, C. Vandensteendam, Cathodic dissolution in the electrocoagulation process using aluminium electrodes, J. Environ. Monit., 2 (2000) 77–80.
[60] J.N. Hakizimana, B. Gourich, M. Chafi, Y. Stiriba, C. Vial, P. Drogui, J. Naja, Electrocoagulation process in water treatment: a review of electrocoagulation modeling approaches, Desalination, 404 (2007) 1–21.
[61] D.O. Siringi, P. Home, J.S. Chacha, E. Koehn, Is electrocoagulation (EC) a solution to the treatment of wastewater and providing clean water for daily use, ARPN J. Eng. Appl. Sci., 7 (2012) 197–204.
[62] D. Lakshmanan, D.A. Clifford, G. Samanta, Ferrous and ferric ion generation during iron electrocoagulation, Environ. Sci. Technol., 43 (2009) 3853–3859.
[63] M. Chafi B. Gourich, A.H. Essadki, C. Vial, A. Fabregat, Comparison of electrocoagulation using iron and aluminium electrodes with chemical coagulation for the removal of a highly soluble acid dye, Desalination, 281 (2011) 285–292.